Linked Regularities in the Development and Evolution of Mammalian Brains

Barbara L. Finlay* and Richard B. Darlington

Analysis of data collected on 131 species of primates, bats, and insectivores showed that the sizes of brain components, from medulla to forebrain, are highly predictable from absolute brain size by a nonlinear function. The order of neurogenesis was found to be highly conserved across a wide range of mammals and to correlate with the relative enlargement of structures as brain size increases, with disproportionately large growth occurring in late-generated structures. Because the order of neurogenesis is conserved, the most likely brain alteration resulting from selection for any behavioral ability may be a coordinated enlargement of the entire nonolfactory brain.

If a species undergoes strong selection pressure for the optimization of a behavioral ability that depends on the size of a localized functional system in the brain, what changes take place in the organization of the brain as a whole? Because brain tissue is metabolically expensive, the need for energetic efficiency should result in the most localized possible increase in brain volume corresponding to the behavioral adaptation. However, required computational structures or the nature of existing developmental programs could severely constrain the range of local adaptations; examples of such factors include cross-organism maturational "clocks" and trophic relations between developing organs. Gould has argued eloquently for the need to consider the roles of both specific adaptations and developmental constraints in determining the paths of evolution (*1*). Conservatism has been the emerging theme of many genetic analyses of the regulation of early embryogenesis in invertebrates and vertebrates (*2*). The study of brain specializations among current mammals and of the accompanying alteration or stability in neurogenesis can yield a formal and quantitative understanding of the range of local adaptations permitted in basic vertebrate neurogenesis and the degree of conservation of fundamental patterns.

Evidence exists both for general organizational constraints and for specific brain adaptations for particular behaviors. Capacity for bird song (*3*) and foraging memory (*4*, *5*), certain sex differences (*6*), hand preference (*7*), and, arguably, the lateralization of the human brain for language (*8*) have been linked to the cell numbers and volumes of particular brain areas. In contrast, a comprehensive study of dexterity in 22 mammalian species representing a wide range of manual dexterity (hooves to hands) produced interesting evidence for general organismal constraints (*9*). Ranked dexterity and the cortical volume devoted to forelimb control were highly related, but dexterity and total cortex volume were equally highly related because the space devoted to forelimb control was almost completely predictable from total cortex size. This work suggests that the amount of cortex devoted to forelimb control can increase only as the result of an apparently inefficient increase in total cortex volume. A similar relation has been found between isocortex size and total brain size (we will use the terms isocortex and allocortex in preference to neocortex and paleocortex, because of the latter terms' inappropriate phylogenetic implications, except when making direct reference to the nomenclature and divisions used in the studies reviewed here). In mammals with large brains, and most notably in humans, the brain becomes disproportionately composed of isocortex (*10*). The volume of the isocortex is very closely predictable, by an exponential function, from total brain size across a wide range of species (*11*). To explore the relative magnitude of size changes in neural structures attributable to general constraints on brain development versus those attributable to specific adaptation, we used published information about brain sizes and patterns of brain neurogenesis in various mammalian species.

Scaling Species and Structure Sizes

The developmental constraint hypothesis suggests that it should be possible to predict the size of any neural structure in any spe-

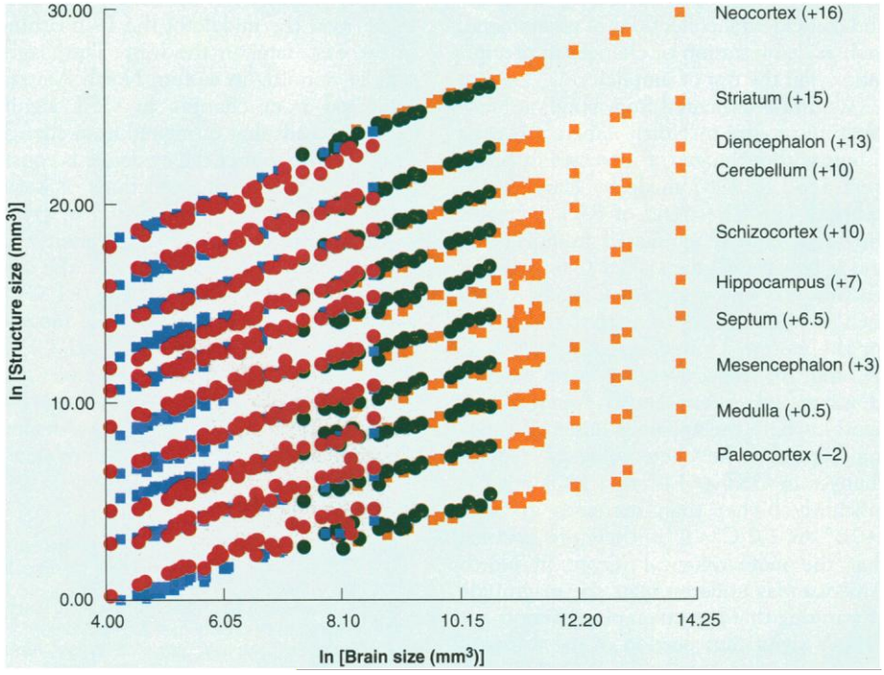

Fig. 1. Sizes of 10 measured brain subdivisions from 131 species plotted as a function of total brain size (orange squares, simians; green circles, prosimians; red circles, insectivores; and blue squares, bats). This method of representation emphasizes the linearity of the relation between brain sizes and structure sizes across mammalian groups on logarithmic scales. Each scatterplot of data points corresponds to a brain subdivision. Arbitrary constants (in parentheses after each subdivision name) were added to separate the plots visually; their normal overlap can be seen in Fig. 2A. Table 1 lists the slopes and intercepts of each regression equation for each structure.

The authors are in the Department of Psychology, Uris Hall, Cornell University, Ithaca, NY 14853, USA.

*To whom correspondence should be addressed.

cies from a simple rule, whereas the adaptation hypothesis implies that no such rule could apply. Therefore, a way to assess these competing views is to attempt to derive such a rule and to see how widely and accurately it works. For this purpose, we used data collected for allometric analysis (*12*) on the adult volumes of 12 nonoverlapping brain divisions for 131 mammals: 40 insectivores, 43 bats, 21 prosimians, and 27 simians including *Homo sapiens*. Advantages of this data set include the large numbers of species, the wide range of niches (including terrestrial, arboreal, fossorial, amphibious, and flying), the wide range of brain sizes (58.4 to 1,252,000 mm^3) and body weights (1.86 to 105,000 g), and the fact that these structures constitute the entire brain. Because of the wide range of sizes involved, we used logarithms of absolute sizes in all our analyses. (We omitted the accessory olfactory nucleus from our analyses because it is by far the smallest of the 12 structures characterized and is given a value of zero in 14 of the 131 species.)

Of the remaining 11 structures, on logarithmic scales the sizes of all structures correlated 0.960 or higher with total brain size, except for the main olfactory bulb, for which this correlation was only 0.696. Table 1 describes the 10 nonolfactory structures, and Fig. 1 shows their sizes plotted as functions of total brain size, with all variables on natural logarithmic scales. The plots show a high correlation within each structure and indicate the continuity of structure sizes across the orders (insectivores, bats, and primates) and suborders (simians and prosimians). The regression lines running through these plots are not exactly parallel; we have arranged the 10 plots in order of their regression slopes, with the largest slope (for the neocortex) on top.

We replotted the same data (Fig. 2A) to emphasize how the relative sizes of brain structures change across species. The arbitrary constants added in Fig. 1 are now removed, and a third axis is added to show the volume of the structures (in cubic millimeters) without the logarithmic transformation. This axis shows how the neocortex quickly expands in volume relative to other structures as brain size increases, despite the linearity of the relations in Fig. 1.

A Two-Factor Model of Structure Size

When a principal components analysis was applied to the covariance matrix of the 11 logarithmically transformed structure sizes, the first principal component accounted for 96.29% of the total variance. This factor is essentially brain size; across the 131 species the two variables correlated 0.9980. When brain size and its square (to account for any residual nonlinearities) were used to predict the sizes of individual brain parts, they explained 96.84% of the variance. Thus, the finding of Hofman (*11*) that there is a highly predictable relation between isocortex size and total brain size applies to all major brain subdivisions except the olfactory bulb. Positive correlations between

Table 1. Components of brain divisions analyzed by Stephan *et al.* (*12*) and regression equation values (*b*, slope; *a*, intercept) for change in structure size across species.

Structure	Slope	Intercept	Components
Paleocortex	0.249	4.719	Pyriform lobe
Medulla	0.259	4.976	Includes substantia reticularis
Mesencephalon	0.266	4.523	Without substantia reticularis
Septum	0.280	2.875	Septum pellucidum, septum verum, diagonal band of Broca, bed nucleus of anterior commissure
Hippocampus	0.281	4.977	All
Schizocortex	0.292	3.725	Entorhinal, perirhinal, presubicular, and subicular cortices with underlying white matter
Cerebellum	0.341	5.493	Cerebellum proper, brachium and nuclei pontis
Diencephalon	0.344	4.873	Includes globus pallidus; hypophysis excluded
Striatum	0.353	3.53	Caudate, putamen, nucleus accumbens, and internal capsule; not globus pallidus
Neocortex	0.445	6.148	Includes white matter and corpus callosum

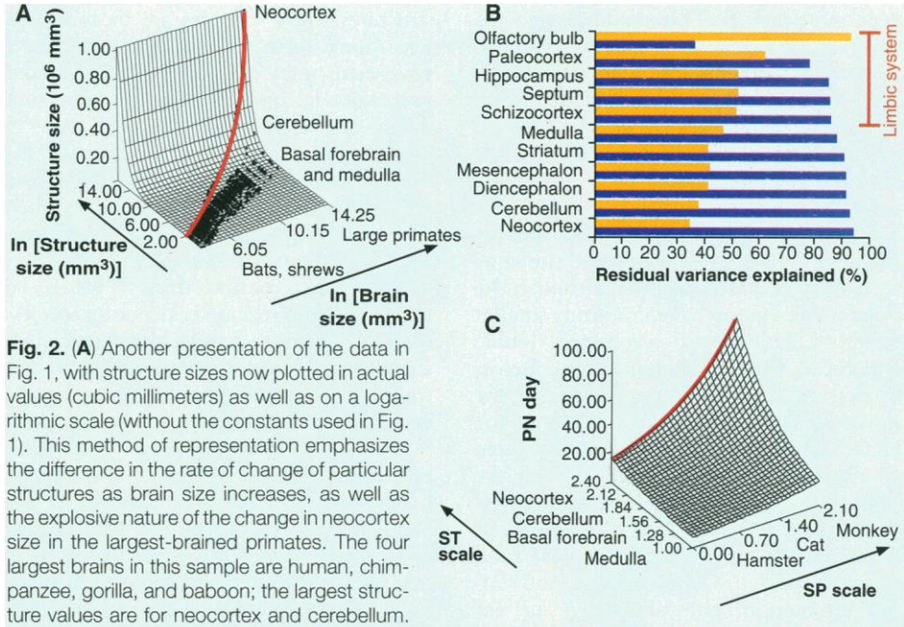

Fig. 2. (**A**) Another presentation of the data in Fig. 1, with structure sizes now plotted in actual values (cubic millimeters) as well as on a logarithmic scale (without the constants used in Fig. 1). This method of representation emphasizes the difference in the rate of change of particular structures as brain size increases, as well as the explosive nature of the change in neocortex size in the largest-brained primates. The four largest brains in this sample are human, chimpanzee, gorilla, and baboon; the largest structure values are for neocortex and cerebellum. Structures and species listed along the horizontal and vertical axes are placed approximately to illustrate the dimensions scaled. The red line highlights the change in neocortex volume across species. (**B**) Relative loadings of the two factors of the principal components analysis on the 11 brain divisions. The first factor (blue bars), which is most highly correlated with the neocortex, loads strongly on all structures but the olfactory bulb and accounts for 96.29% of the total variance. The second factor (yellow bars) is most highly correlated with the olfactory bulb and loads more strongly on structures with a major limbic component (bracketed); it accounts for 3.00% of the variance. The diencephalon has both limbic and nonlimbic components. (**C**) Model of the prediction of ln (PN day − 7) from the SP and ST scales for seven mammalian species. The SP scale ranks the total duration of neurogenesis across the seven species (from lowest to highest, hamster, mouse, rat, spiny mouse, possum, cat, and monkey). The ST scale ranks the order of neurogenesis across the 51 structures, with the lowest value for cranial motor nuclei and the highest values for retinal bipolar cells and cortical layer II–III. The red line shows the change in the timing of neocortex generation across the seven species, corresponding to the red line in (A).

most brain structures and total brain size have been reported (*13*); we stress here the pervasive and nonlinear nature of these relations (Fig. 2A). When body size was substituted for brain size in the quadratic regression, the explained percentage of variance dropped to 94.35%. Thus, one way to think about brain structure is to assume that the overwhelming proportion of the total variance in individual structure sizes is explained by the single factor of overall size, which is more usefully construed as brain size than as body size. The major factor controlling brain size is the rate and duration of cell division; this topic is further explored below.

In this principal components analysis, the percentages of variance explained by the first four components were 96.29, 3.00, 0.21, and 0.16%, respectively. The last three terms all seem very small compared to the first. However, the second term is more than 14 times the third term, and its value of 3.00% is 81% of the 3.71% unexplained by the first factor. Because 81% of otherwise unexplained variance could be explained by adding a single term to the model, we did so. The third term is only slightly larger than the fourth term, so it is difficult to justify the addition of a third factor without adding a fourth or even more factors. This analysis suggests a two-factor model.

After a standard rotation of the principal components, one factor loaded highly on the isocortex and a second factor loaded highly on the olfactory bulb (Fig. 2B). The second factor also loaded relatively highly on all the structures with a classic "limbic" component. All three orders, insectivores, bats, and primates, showed the same second factor independently, although the primates as a group have uniformly smaller olfactory bulbs and associated limbic structures. We then simplified the factors by defining one factor as the size of the isocortex and the other as the size of the olfactory bulb, with all variables measured on natural logarithmic scales. When the sizes of individual structures were predicted from second-order regression equations containing the predictors of isocortex and olfactory bulb sizes, their squares, and simple interaction, the percentage of explained variance was 99.19%, essentially the same percentage as explained by the first two principal components.

This two-factor model provides an even more accurate description of brain configuration than did the previous one-factor model. The typical (root mean square) error in predicting an individual structure from this model is only 0.187. Because all variables are measured on natural logarithmic scales, this means that the typical structure is estimated with an error of about 20% of its true size. This error variance includes species-specific adaptation but also includes random measurement error plus individual variation within a species; in the Stephan *et al.* data set (*12*), each species is typically represented by just one individual. Thus it is safe to say that in the three orders studied here, simple across-species generalizations account for far more of the variance in individual structure size than can be attributed to any other factor, including species-specific adaptation.

How can we reconcile this evidence for cross-species conservatism in patterns of brain enlargement with the strong intuition and evidence that species-specific brain adaptations must exist? There are several answers. First, the structures considered here are broad brain divisions, and reallocation of functions may occur within these divisions. Second, brains vary on other dimensions including connectivity, cell morphology, and neurotransmitter complements. Third, the enormous range of structure sizes across species is important for the following reason: In a moderate-sized sample, a normally distributed variable typically has a total sample range of about five times its standard deviation. In predicting the size of brain structures, as noted above, the standard deviation of predictive errors is 0.187 averaged across structures when variables are measured on logarithmic scales. This suggests that for a typical structure, two species identical on our two major factors may have structure sizes differing by as much as 5×0.187 or 0.935 on a logarithmic scale. Because $\exp(0.935) = 2.55$, individual structures may differ by a factor of as much as 2.5 in size, even when the two species being compared are very similar on the two major factors. Inspection of the raw data confirms this conclusion. To the investigator seeking evidence for species-specific adaptation, a twofold difference in a structure's volume is striking, even if it is trivial in comparison to the total range of size of that structure and small in comparison to the range of structure size with body size held constant. For instance, the human brain is some 21,400 times the size of the brain of the smallest shrew, and the human neocortex is some 142,000 times larger than that of the shrew. For a squirrel monkey (*Saimiri sciureus*) and an insectivore (*Tenrec ecaudatus*) of comparable body size, the brain weight of the squirrel monkey is about 10 times greater than that of the tenrec, and its isocortex is about 60 times larger (*12*). These broad ranges allow noticeable amounts of species-specific variation in structure size despite the high cross-species correlations among the sizes of various neural structures. Comparing the neocortex to other structures, a modest relative change in total brain size produces large relative changes in neocortex size due to the enormous leverage of the exponential function linking the two (represented by the red line in Fig. 2A). This source of variation is often "factored out" in studies of specific brain adaptation. The next section considers the physical or developmental causes of differences in the growth rates of structures as a function of total brain size.

Effect of the Duration of Neurogenesis on Structure Size

The number of neurons in a structure can be increased by increasing the rate at which its neuronal precursors are produced (*14*), increasing the length of time over which they are produced, decreasing the rate of neuronal death, or any combination thereof. Variations in all these factors occur between species, and all contribute to the final number of neurons. However, because a given structure may be thousands of times larger in one species than in another, the only factor that can plausibly produce differences of this magnitude is the duration of neurogenesis. An additional 17 doublings of a structure's precursor cells can yield some 131,000 times the final number of neurons; this is roughly equivalent to the aforementioned difference between the isocortex sizes of humans and shrews.

During early brain development, precursor cells for neurons, located for the most part on the ventricular surface of the neural tube, undergo symmetric division, each cell producing two daughter cells that may divide again and again. The precursor pool thus increases by an exponential function appropriate to the rate of cell division and the number of precursor cells. Neurons are said to have their "birthday" when a precursor cell undergoes an asymmetric division and the resulting neuroblast exits the precursor pool and differentiates as a neuron. The peak of neuronal birthdays in a neural structure is a measure of the duration of cytogenesis for that structure: The longer neurogenesis is delayed, the more precursor cells can be formed and the larger the structure that results. Because we considered the duration of neurogenesis (as measured by peak neurogenesis) to be a likely determinant of structure size, we investigated whether a simple model similar to the one described for structure size could be developed to relate schedules of neurogenesis across species and to allow a ranking of changes in structure size as a function of brain size.

A second database was gathered from the primary literature; it consists of the number of days from conception to peak neurogenesis, as measured by tritiated thymidine autoradiography, in seven different mammals for 51 brain subdivisions (Table 2). Our sample included four rodents, one

Table 2. Peak day of neurogenesis for individual species and structures, with reference numbers (in parentheses).

Structure	Rhesus monkey	Rat	Mouse	Cat	Possum	Spiny mouse	Hamster
Cranial motor nuclei		12 (*34*)	9 (*15*)				
Cranial sensory nuclei		13 (*34*)	11 (*16*)				
Vestibular nuclei		13 (*35*)					
Cochlear nuclei		15 (*35*)	12 (*17*)		31 (*58*)		
Purkinje cells	39 (*65*)	15 (*36*)	10.5 (*18*)		22 (*59*)		
Deep cerebellar nuclei	38 (*65*)	14 (*37*)					
Inferior olivary nucleus		13 (*38*)	10 (*15*)				
Pontine nuclei		17 (*37*)	13.5 (*19*)				
Red nucleus		13 (*38*)					
Locus ceruleus	32 (*66*)	12 (*39*)					
Raphe complex	30 (*66*)	13 (*39*)	13.5 (*19*)				
Inferior colliculus	43 (*66*)	17 (*40*)			25 (*58*)		
Superior colliculus	41 (*66*)	16 (*41*)	13 (*20*)		29 (*58*)		12 (*54*)
Substantia nigra	39 (*66*)	16 (*41*)					
Lateral geniculate nucleus	43 (*67*)	15 (*42*)	12 (*21*)	27 (*60*)	26 (*58*)		
Ventrolateral geniculate nucleus		15 (*42*)	11.5 (*22*)	26 (*60*)			
Reticular nuclei		14 (*42*)	11 (*21*)	24 (*60*)			
Medial geniculate nucleus		14 (*42*)	11 (*21*)	26 (*60*)	26 (*58*)		
Ventroposterolateral and ventrobasal nuclei		15 (*42*)	12.5 (*21*)				
Anteroventral, anteromedial, and anterodorsal nuclei		16 (*42*)	13.5 (*21*)				
Suprachiasmatic nucleus		15 (*43*)	13 (*21*)	25 (*61*)	22 (*58*)		10 (*55*)
Preoptic nucleus		13 (*43*)	12.5 (*22*)				
Septal nuclei	45 (*68*)	15 (*44*)	13 (*22*)			19 (*53*)	
Amygdala	38 (*69*)	15 (*45*)	12 (*23*)			18 (*53*)	
Caudoputamen	45 (*70*)	15 (*46*)	14 (*25*)		29 (*59*)	20 (*53*)	
Globus pallidus		14 (*46*)	11 (*23*)		22 (*59*)		
Claustrum			12.5 (*23*)		22 (*59*)	18 (*53*)	
Isles of Calleja			16 (*22*)				
Nucleus accumbens	45 (*68*)	19 (*46*)	16 (*22*)			22 (*53*)	
Magnocellular basal forebrain	30 (*71*)						
Dentate gyrus	48 (*72*)	17 (*47*)				22 (*53*)	
CA 1-2	48 (*72*)	19 (*47*)	15 (*24–26*)			20 (*53*)	
Presubiculum	48 (*72*)	18 (*47*)	13.5 (*27*)				
Parasubiculum	48 (*72*)	17 (*47*)	13.5 (*27*)				
Subiculum	48 (*72*)	17 (*47*)	13 (*27*)			20 (*53*)	
Entorhinal cortex	48 (*72*)	15 (*47*)	13 (*27*)			20 (*53*)	
Retinal ganglion cells	43 (*73*)	17 (*48*)	13 (*28*)	30 (*62*)			12 (*56*)
Retinal amacrine cells	56 (*73*)	17 (*48*)	15 (*29*)	45 (*62*)			14 (*56*)
Retinal bipolar cells	85 (*73*)			65 (*62*)			
Retinal horizontal cells	40 (*73*)			30 (*62*)			
Cones	56 (*73*)		14 (*30*)	36 (*62*)			
Rods	85 (*73*)		19 (*30*)	65 (*62*)			
Anterior olfactory nucleus		14 (*49*)	13.5 (*31*)			22 (*53*)	
Nucleus of lateral olfactory tract		15 (*49*)	12.5 (*31*)				
Mitral cells		15 (*50*)	12 (*32*)			18 (*53*)	
Tufted cells		18 (*50*)	16 (*32*)			22 (*53*)	
Subplate	43 (*74*)	15 (*51*)	11 (*33*)	24 (*63*)	22 (*58*)	14 (*53*)	11 (*57*)
Cortical layer VI	53 (*75*)	17 (*52*)	12.5 (*33*)	23 (*64*)	38 (*58*)	18 (*53*)	12 (*57*)
Cortical layer V	70 (*75*)	17 (*52*)	13 (*33*)	35 (*64*)	45 (*58*)	20 (*53*)	14 (*57*)
Cortical layer IV	80 (*75*)	18 (*52*)	17 (*33*)	39 (*64*)	49 (*58*)	20 (*53*)	15 (*57*)
Cortical layer II–III	90 (*75*)	19 (*52*)	15 (*33*)	56 (*64*)	67 (*58*)	29 (*53*)	16 (*57*)

carnivore, one marsupial, and one primate. Although the availability of these birthdating data by species was not under experimental control, four major radiations are represented, and two of the rodent species were deliberately chosen by the original investigators for neural birthdating because of their very short and very long gestational periods compared to the rodent mean. The rodents include the mouse (*Mus musculus*) (*15–33*), the laboratory rat (*Rattus norvegicus*) (*34–52*), the spiny mouse (*Acomys cahirinus*) (*53*), and the hamster (*Mesocricetus auratus*) (*54–57*) (Table 2). The mouse and rat are both intermediate in gestational period and maturational state at birth, differing only in size. By comparison, the hamster has one of the shortest gestational periods and one of the most rapid rates of maturation of all eutherian mammals, whereas the spiny mouse has a long gestational period and is quite precocial at birth. The brush-tailed possum (*Trichosurus vulpecula*) is the sole marsupial of the group (*58, 59*). The domestic cat (*Felis catus*) represents the radiation Carnivora; for this species, principally visual system structures have been birthdated (*60–64*). Finally, the rhesus monkey (*Macaca mulatta*) has the largest brain, the most corticalization, and the longest gestational period of this group (*65–75*).

The 51 structures studied ranged from primary motor and secondary sensory neurons in the caudal hindbrain to the neocortex and olfactory bulb, and they represent smaller divisions of the brain than those in the first database. The studies yielded a total of 174 dates of peak neurogenesis for these structures, or just under half of the 7 × 51 potential values shown in Table 2. Data on the peak day of neurogenesis were gathered from the literature in a maximally inclusive rather than an exclusive fashion. If quantitative data were given, the peak day was taken directly from the tables or graphs and summed over subdivisions or spatial gradients as necessary (for example, by combining data on various nuclei of the amygdala into a single peak value for Amygdala). If the data were represented as labeled cells on brain sections, they were counted and the peak value was taken directly. In some cases, the author simply stated a peak day. All neurogenesis days are given as days after conception. For all rodents, the day after mating was counted as day 0. Although data were available for granule cells in three structures (the cerebellum, hippocampus, and olfactory bulb), they are omitted from this analysis because of the difficulty of fixing starts, peaks, and ends to their protracted genesis; this omission has both substantive and methodological importance, as noted below.

Because our 7 × 51 table of structure birthdates was only about half full, we con-

strued the data as a 7 × 51 analysis of variance table and then applied a general linear model to the data. This modeling approach gives each species a score on a species scale (SP) and gives each structure a score on a structure scale (ST), such that the peak day of neurogenesis is predicted as well as possible from the scores $SP + ST$. An alternative description is that the method attempts to fill in the empty cells of the data table; then, except for an additive constant, *SP* and *ST* are simply the row and column means of the filled-in table.

As expected, hamster had the lowest score on the SP scale, indicating fastest neurogenesis, whereas rhesus monkey had the highest. By trial and error, we could maximize predictive accuracy by predicting not the peak day of neurogenesis (PN day) itself, but rather $Y = \ln(\text{PN day} - 7)$. As described below, we believe this function makes good sense in the context of early events in embryogenesis. After deriving these scales, we found that a slight modification to the model yielded better overall fit. Relative to the six placental species, the nonplacental possum's neurogenesis was more protracted than would be predicted by the possum's position on the SP scale. For the possum, the model was modified such that the prediction was $SP + 1.673ST$. With this modification, across the seven species and 174 data points, the correlation between observed and predicted Y values was 0.988.

The model's prediction of PN day as a function of the SP and ST scales is shown in Fig. 2C. Note that although the curve accelerates, it is not as "explosive" as that in Fig. 2A. The most likely reason for this difference is an additional nonlinear relation between PN day (the vertical axis of Fig. 2C) and structure size (the vertical axis of Fig. 2A). This relation is exponential if precursor cells multiply exponentially over time.

The function $Y = \ln(\text{PN day} - 7)$ was chosen because this function is most accurately predicted from the SP and ST scales. In retrospect, however, it seems reasonable that the prediction of peak neurogenesis has a constant and an exponential component. After conception in all mammalian species, early organizational events such as implantation, blastulation, and differentiation of the basic germinal layers of the embryo must occur before the nervous system begins to develop. This analysis suggests that these events occur during the first 7 postconceptional days and that this period is roughly constant across these species. Thereafter, neural structures appear to develop on an exponential timetable, yielding the particular Y function we discovered.

Integrating Results on Structure Size and Neurogenesis

The corresponding regularities of structure size and order of neurogenesis suggest that they are somehow related (Fig. 2, A and C). Can the pattern of neurogenesis predict which structures grow proportionately larger or smaller as brain size increases? The answer cannot be easily obtained because researchers studying neurogenesis have been interested in single structures, whereas allometric analyses have primarily used brain subdivisions that include many structures. However, we found additional data on cross-species sizes of seven structures (*12*) for which we had previously computed an *ST* score: septal nuclei, caudoputamen, neocortex (weighted mean of birthdates of layers VI–II), lateral geniculate nucleus, globus pallidus, amygdala, and vestibular nuclei. Seventy-six species had been studied and data were available for 370 of the 76 × 7 = 532 possible entries. For each of these seven structures, we fitted a simple linear regression predicting the logarithm of structure size from the logarithm of brain size. As before, fits were very good; the structure sizes correlated 0.970 to 0.992 with total brain size.

A linear regression is defined by two parameters: the slope *b* and the intercept *a*. The larger the structure size, the larger the value of *a*, *b*, or both. We treated the seven sets of *a* and *b* values as predictor variables (varying across structures) in a two-variable multiple regression that predicted the structure's position on the ST scale, and we found a correlation of 0.943 between the *ST* score (scaling of order of neurogenesis) and the combined slope and intercept of the change in size of the same structures with brain size. As predicted, the coefficients of both these variables were positive. Thus, structures that grow disproportionately large as brain size increases have late birthdates, which allow a longer period for generation of their precursor pool.

Can evidence be found for a biological mechanism that would account for the second factor in our original analysis of structure sizes, which loaded most highly on the olfactory bulb and secondarily on limbic structures such as the allocortex, hippocampus, and septum? Using $\ln(\text{PN day} - 7) = SP + ST$, we computed *ST* values for the start and end of neurogenesis for as many structures as possible for the rhesus monkey (which has a smaller-than-average-mammal olfactory bulb and limbic system). We then used these *ST* values to derive PN day values with the rat *SP* values, which enabled us to transform the postconceptional day timetable of the monkey to that of the rat so that we could directly compare the details of their neurogenesis. In Fig. 3, structures have been grouped into rough functional systems. The limbic system begins its terminal neurogenesis prematurely and synchronously in the monkey compared with the rat, and these factors alone could account for the smaller relative size of the monkey limbic system. It is possible that this system may be "addressable" as a functional subsystem within the brain during development: The list of structures with

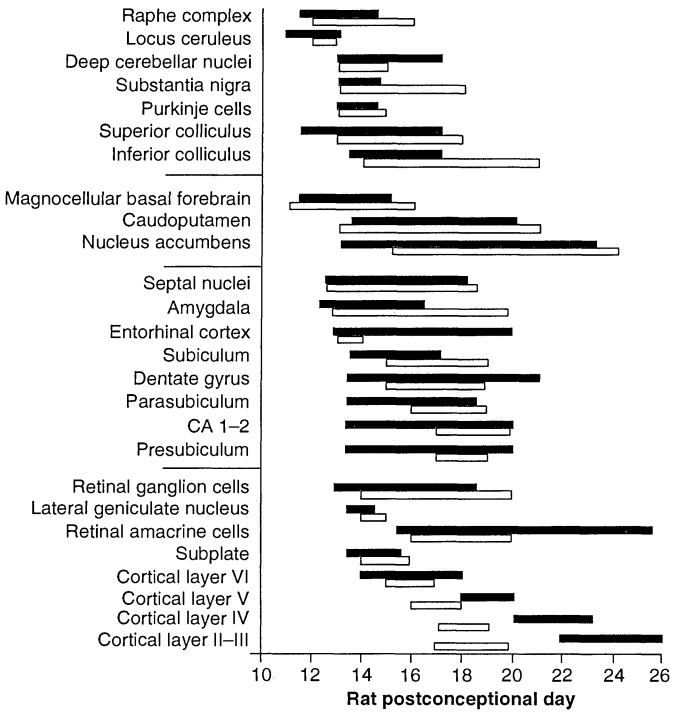

Fig. 3. Measured duration of terminal neurogenesis for 26 neural structures in monkey (solid bars), transformed to rat postconceptional days (open bars) for direct comparison by means of the derived formula $\ln(\text{PN day} - 7) = SP + ST$. The relative duration of the period in which neurons undergo their final division is comparable in monkey and rat neurogenesis. Limbic structures (septum through presubiculum) in the monkey undergo an early and relatively synchronous birth compared to those in the rat. For the last generated layers of the isocortex, there is residual uncorrected nonlinearity between the rat and monkey schedules. The dissimilarity of the durations of amacrine neurogenesis could reflect the inclusion of two cell classes in monkey and only one in rat.

premature neurogenesis overlaps with those labeled by the limbic system–associated membrane protein (LAMP) factor in both adults and neonates (*76*).

Qualifications and Conclusions

In a model as broad as this, it is important to note the limitations of the data available and the kinds of conclusions that can be reached. This model is only defined for mammals, in which neurogenesis is for the most part confined to early development and for which it is meaningful to define a peak day of neurogenesis. Other vertebrates, including cartilaginous and bony fish, amphibians, reptiles, and birds, continue neurogenesis throughout their lifetimes, with distinct patterns associated with metamorphosis, sexual maturation, and seasonal changes. It would thus be interesting to examine a range of nonmammalian vertebrates to see whether they exhibit less consistency in the relative sizes of brain subdivisions compared to total brain size; appropriate data have been gathered for a number of birds (*77*) and teleosts (*78*).

The cross-mammalian generalizability of our results is supported by the fact that the order of neurogenesis in a data set of one marsupial, four rodents, a carnivore, and a primate predicts structure sizes in a separate data set of primates, bats, and insectivores. Because of the relative absence of marsupials and carnivores and the complete absence of ungulates, caution should be exercised in the extension of this model to all mammals, although isocortex size scales with brain size in selected representatives of these orders (*79*). Examination of additional species in specialized niches, or in specific structures close to the sensory periphery, would provide the strongest test of developmental constraint in neural evolution. This analysis is applicable to sirenians (*80*) and cetaceans (*81*).

Of course, specific adaptations of brain structures to behavior have been reported, and they often involve developmental processes explicitly neglected by this model. Protracted or continuing neurogenesis, such as in the hippocampus of foraging birds and mammals (*5*) or the song control nuclei of birds (*82*), constitutes one such process. Our model omits from the analysis granule cells of all kinds, which characteristically have protracted neurogenesis. Neuronal death or other regressive events are often imposed on an originally homogenous population to produce sexual dimorphisms (*6*). The variation in structure sizes seen in these studies represents a twofold to threefold difference, which is the range of "error" in our model. The path of brain evolution may thus depend on which cell types in a given structure are critical to a selected behavior and whether protracted generation or death is part of their developmental repertoire.

We might distinguish two types of brain evolution, one "easy" and one "difficult." In the easy mode, modifications are made only to total duration of development. Small variations in developmental duration might occur so commonly, and have such major leverage on the relative sizes of brain components, that they may be the principal basis of variation in structure sizes on which selection may operate. Modifications of this type to the developmental clock have occurred so often that even within the class Mammalia, whose living members all share a common ancestor within the last 250 million years, some neural structures (notably the isocortex) differ in size by a factor of more than 200 after adjusting for differences in body size (*83*). By contrast, a coordinated enlargement of many independent components of one functional system without enlargement of the rest of the brain may be more difficult, as its probability would be the vanishingly small product of the probability of each component enlarging individually.

What is the significance of a conserved order but a nonlinear scaling of neurogenesis for mammalian evolution generally? If an animal were strongly selected for the ability to make accurate computations for auditory localization, which in turn depends on the number of neurons in the inferior colliculus, the most readily available variation might be the crude one of changing the duration or the gross rate of neurogenesis for the entire brain, which would open the possibility of extensive pleiotropic effects on many behavioral capacities consequent to selection on one behavioral trait. For human evolution in particular, theories that start from a primary behavioral trait appear to account for human evolution many times over. Dexterity and tool use, language, group hunting, various aspects of social structure, and the ability to plan for the future have all been proposed as primary in the cascade of changes leading to the constellation of traits we now possess. The location of large primates on the neocortex curve where small relative changes in brain size are associated with large relative changes in isocortex size (Fig. 2A) may explain the multiple facets and rapid rate of human evolution. The highly conserved sequence of events in neurogenesis provides a reason why selection for any one ability might cause, in parallel, greater processing capacity for all the others. This observation strengthens the case for the isocortex as a general-purpose integrator that allows the organism to take advantage of the extra brain structure in ways not directly selected for during evolution.

REFERENCES

1. S. J. Gould, *Ontogeny and Phylogeny* (Harvard Univ. Press, Cambridge, MA, 1977).
2. C. Nüsslein-Volhard, *Science* **266**, 572 (1994); J. Kimble, *ibid.*, p. 577; N. H. Patel, *ibid.*, p. 581.
3. F. Nottebohm, C. Pandazis, S. Kasparian, *Brain Res.* **213**, 99 (1981); T. J. DeVoogd, J. R. Krebs, S. D. Healy, A. Purvis, *Proc. R. Soc. London Ser. B Biol. Sci.* **254**, 75 (1993).
4. J. R. Krebs, *Philos. Trans. R. Soc. London Ser. B Biol. Sci.* **329**, 161 (1990).
5. D. F. Sherry, L. F. Jacobs, S. J. C. Gaulin, *Trends Neurosci.* **15**, 298 (1992).
6. D. R. Sengelaub, in *Advances in Comparative and Environmental Physiology*, J. Balthazart, Ed. (Springer-Verlag, Berlin, 1989), vol. 3, pp. 239–267.
7. D. Purves, L. E. White, T. J. Andrews, *Proc. Natl. Acad. Sci. U.S.A.* **91**, 5030 (1994).
8. N. Geschwind and W. Levitsky, *Science* **161**, 186 (1968); A. M. Galaburda, J. Corsiglia, G. D. Rosen, G. F. Sherman, *Neuropsychologia* **25**, 853 (1987).
9. R. J. Nudo and R. B. Masterson, *J. Comp. Neurol.* **296**, 584 (1990).
10. H. J. Jerison, *Evolution of the Brain and Intelligence* (Academic Press, New York, 1973); ———, in *The Neocortex: Ontogeny and Phylogeny*, B. L. Finlay, G. Innocenti, H. Scheich, Eds. (Plenum, New York, 1991), vol. 200, pp. 5–20.
11. M. A. Hofman, *Prog. Neurobiol.* **32**, 137 (1989).
12. H. Stephan, H. Frahm, G. Baron, *Folia Primatol.* **35**, 1 (1981).
13. H. D. Frahm, H. Stephan, M. Stephan, *J. Hirnforsch.* **23**, 375 (1982); G. Baron, H. D. Frahm, H. Stephan, *ibid.* **29**, 509 (1988).
14. C. Dehay, P. Giroud, M. Berland, I. Smart, H. Kennedy, *Nature* **366**, 464 (1993).
15. E. Taber, *Anat. Rec.* **145**, 291 (1963).
16. E. T. Pierce, *J. Comp. Neurol.* **131**, 27 (1970).
17. ———, *Anat. Rec.* **166**, 388 (1970).
18. I. L. Miale and R. L. Sidman, *Exp. Neurol.* **4**, 277 (1961); L. L. Uzman, *J. Comp. Neurol.* **114**, 137 (1960).
19. E. T. Pierce, *J. Comp. Neurol.* **126**, 219 (1967).
20. G. R. DeLong and R. L. Sidman, *ibid.* **118**, 205 (1962).
21. A. M. Johnston and J. B. Angevine, *Anat. Rec.* **154**, 163 (1966).
22. E. S. Creps, *J. Comp. Neurol.* **157**, 161 (1974).
23. R. L. Sidman and J. B. Angevine, *Anat. Rec.* **142**, 327 (1962); J. A. McConnell, *ibid.* **181**, 418 (1975).
24. V. S. Caviness, *J. Comp. Neurol.* **151**, 113 (1973).
25. J. B. Angevine and J. A. McConnell, *Anat. Rec.* **178**, 300 (1974).
26. J. B. Angevine, *ibid.* **148**, 255 (1964); *Exp. Neurol. Suppl.* **2**, 1 (1965); B. B. Stanfield and W. M. Cowan, *J. Comp. Neurol.* **185**, 423 (1979).
27. V. S. Caviness and R. L. Sidman, *J. Comp. Neurol.* **148**, 141 (1973).
28. U. Drager, *Proc. R. Soc. London Ser. B Biol. Sci.* **224**, 57 (1985).
29. R. L. Sidman, in *The Structure of the Eye*, G. K. Smelser, Ed. (Academic Press, New York, 1961), pp. 487–506.
30. L. D. Carter-Dawson and M. M. LaVail, *J. Comp. Neurol.* **188**, 263 (1979).
31. E. S. Creps, *ibid.* **157**, 139 (1974).
32. J. W. Hinds, *ibid.* **134**, 287 (1968).
33. V. S. Caviness, *Dev. Brain Res.* **4**, 293 (1982).
34. J. Altman and S. A. Bayer, *J. Comp. Neurol.* **194**, 1 (1980).
35. ———, *ibid.*, p. 877.
36. ———, *ibid.* **179**, 23 (1978).
37. ———, *ibid.*, p. 49.
38. ———, *ibid.* **198**, 677 (1980).
39. ———, *ibid.* **194**, 905 (1980).
40. ———, *Exp. Brain Res.* **42**, 411 (1981).
41. ———, *ibid.*, p. 424.
42. ———, *J. Comp. Neurol.* **188**, 455 (1978).
43. ———, *ibid.* **182**, 945 (1978).
44. S. A. Bayer, *ibid.* **183**, 89 (1979).
45. ———, *ibid.* **194**, 845 (1980).
46. R. Marchand and L. Lajoie, *Neuroscience* **17**, 573 (1986).
47. S. A. Bayer, *J. Comp. Neurol.* **190**, 87 (1980).

48. B. E. Reese and R. J. Colello, *Neuroscience* **46**, 419 (1992).
49. S. A. Bayer and J. Altman, *Prog. Neurobiol.* **29**, 57 (1987); S. A. Bayer, *Int. J. Dev. Neurosci.* **4**, 225 (1986).
50. S. A. Bayer, *Exp. Brain Res.* **50**, 329 (1983).
51. _____ and J. Altman, *Exp. Neurol.* **107**, 48 (1990).
52. _____, *Neocortical Development* (Raven Press, New York, 1991).
53. P. C. Brunjes, D. L. Korol, D. G. Stern, *Neurosci. Lett.* **107**, 114 (1989).
54. W. J. Crossland and C. J. Uchwat, *Dev. Brain Res.* **5**, 99 (1982).
55. F. C. Davis, R. Boada, J. LeDeaux, *Brain Res.* **519**, 192 (1990).
56. D. R. Sengelaub, R. P. Dolan, B. L. Finlay, *J. Comp. Neurol.* **246**, 527 (1986).
57. T. U. Woo, J. M. Beale, B. L. Finlay, *Cereb. Cortex* **1**, 433 (1990).
58. K. J. Sanderson and L. M. Aitken, *Brain Behav. Evol.* **35**, 325 (1990).
59. _____, *ibid.*, p. 339.
60. T. L. Hickey and P. F. Hitchcock, *J. Comp. Neurol.* **228**, 186 (1984).
61. J. M. Wyss and B. Sripanidkulchai, *Dev. Brain Res.* **21**, 89 (1985).
62. E. H. Polley, R. P. Zimmerman, R. L. Fortney, in *Development of the Vertebrate Retina*, B. L. Finlay and D. R. Sengelaub, Eds. (Plenum, New York, 1989), pp. 3–29.
63. M. B. Luskin and C. J. Shatz, *J. Neurosci.* **5**, 1062 (1985).
64. _____, *J. Comp. Neurol.* **242**, 611 (1985).
65. B. B. Gould and P. Rakic, *Exp. Brain Res.* **44**, 195 (1981).
66. P. Levitt and P. Rakic, *Soc. Neurosci. Abstr.* **5**, 341 (1979); M. L. Cooper and P. Rakic, *J. Comp. Neurol.* **202**, 309 (1981).
67. P. Rakic, *J. Comp. Neurol.* **176**, 23 (1977).
68. S. Brand and P. Rakic, *Neuroscience* **5**, 2125 (1980).
69. J. H. Kordower, P. Piecinski, P. Rakic, *Dev. Brain Res.* **68**, 9 (1992).
70. S. Brand and P. Rakic, *Neuroscience* **4**, 767 (1979).
71. J. H. Kordower and P. Rakic, *J. Comp. Neurol.* **291**, 637 (1990).
72. P. Rakic and R. S. Nowakowski, *ibid.* **196**, 99 (1981).
73. M. M. LaVail, D. H. Rapaport, P. Rakic, *ibid.* **309**, 86 (1991).
74. I. Kostovic and P. Rakic, *J. Neurocytol.* **9**, 219 (1980).
75. P. Rakic, *Science* **183**, 425 (1974).
76. P. Levitt, *ibid.* **223**, 299 (1984); _____, E. Pawlak-Byczkowska, H. L. Horton, V. Cooper, in *Neurobiology of Down Syndrome*, C. J. Epstein, Ed. (Raven, New York, 1986), pp. 195–210.
77. G. Rehkamper, H. D. Frahm, K. Zilles, *Brain Behav. Evol.* **37**, 125 (1991).
78. R. Brandstatter and K. Kotrschal, *ibid.* **35**, 195 (1990).
79. M. A. Hofman, *ibid.* **27**, 28 (1985).
80. R. L. Reep and T. J. O'Shea, *ibid.* **35**, 185 (1990).
81. W. K. Schwerdtfeger, H. A. Oelschlager, H. Stephan, *Anat. Embryol.* **170**, 11 (1984).
82. J. A. Paton and F. Nottebohm, *Science* **225**, 1046 (1984).
83. H. Stephan, G. Baron, H. D. Frahm, in *Comparative Primate Biology* (Liss, 1988), vol. 4, pp. 1–38.
84. We thank A. Baernstein, K. Jordan, and L. Hinds for their help with the literature search; J. Niederer and J. Crowley for preparation of figures; and K. Stockton for secretarial help. We thank D. Field, R. Johnston, B. Olshausen, D. Sengelaub, D. Troilo, and J. Crowley for their helpful comments. Supported by NIH grant NS19245 to B.F.

Extreme Discordant Sib Pairs for Mapping Quantitative Trait Loci in Humans

Neil Risch* and Heping Zhang

Analysis of differences between siblings (sib pair analysis) is a standard method of genetic linkage analysis for mapping quantitative trait loci, such as those contributing to hypertension and obesity, in humans. In traditional designs, pairs are selected at random or with one sib having an extreme trait value. The majority of such pairs provide little power to detect linkage; only pairs that are concordant for high values, low values, or extremely discordant pairs (for example, one in the top 10 percent and the other in the bottom 10 percent of the distribution) provide substantial power. Focus on discordant pairs can reduce the amount of genotyping necessary over conventional designs by 10- to 40 -fold.

The power of modern molecular methods for identifying Mendelian disease genes, such as those for cystic fibrosis, Huntington disease, and neurofibromatosis, has been amply demonstrated. The feasibility of these methods for identification of susceptibility genes for non-Mendelian disorders (such as diabetes, multiple sclerosis, and hypertension) remains to be seen. A major problem in searching for such loci is the lack of the simple one-to-one correspondence between gene effect (genotype) and disease outcome (phenotype) that is typical for the Mendelian case. Multiple loci may contribute to susceptibility, with complicated interaction effects among loci. For example, in the non-obese diabetic (NOD) mouse model of human insulin-dependent diabetes (IDDM), evidence for at least 10 susceptibility loci was obtained (*1*), and it appears from human studies that IDDM may be equally complex (*2*).

An important class of traits for study in human genetics are quantitative ones, in which the phenotype is measured on a continuous scale. These may either directly underlie disease classification (such as blood pressure and the associated disease, hypertension; or weight and obesity) or may be considered as a risk factor for a disease state (such as cholesterol and ischemic heart disease). One approach is to identify quantitative trait loci (QTL's) in an appropriate animal model system, and then search for similar associations in humans (*3*).

A problem heretofore in studying the genetics of quantitative traits in humans is the low power of linkage analysis to detect loci contributing to the trait. One commonly employed approach is the robust sib pair design first described by Haseman and Elston (*4*). In this method, the difference in trait values (such as height, weight, or blood pressure) for a pair of sibs is squared (D^2) and examined as a function of the number of alleles that the pair have derived from a common parent [identical by descent (ibd)] at a tested marker locus. When a locus contributing to the variation of the quantitative trait lies near the tested marker locus (in other words, there is linkage between the two loci), there will be a negative regression of D^2 on the number of alleles shared ibd; for sibs sharing two alleles ibd, D^2 will be small, while for sibs sharing no alleles ibd, D^2 will be large. This approach has also been extended to pedigree relationships other than sibs (*5*). However, Blackwelder and Elston (*6*) showed that the proportion of the total variance (heritability) in a trait attributable to a contributing locus would need to be large (~50%) to detect linkage in a reasonably-sized sample by sib pair analysis when the sibs are sampled at random (irrespective of their trait values). For example, 2953 pairs would be needed to detect linkage with 90% power for a locus that is responsible for 30% of the variation (30% heritability) (*6*). Extensions of the sib pair approach to allow for multipoint analysis with flanking marker loci have increased the power of this method (*7*). However, even with multipoint analysis, thousands of sib pairs are required to detect linkage to a locus that has a heritability of 25% (*8*).

The fact that power to detect linkage can be increased by using selected versus random samples has recently been noted (*9–10*). This approach is also based on sib pair analysis, but in this case one of the sibs is ascertained to have an extreme value (say, within the top 5 or 10% of the distribution); the second sib is selected at random. Again, regression is the statistical method employed. In this case, however, the value of

N. Risch was in the Department of Epidemiology and Public Health, Department of Genetics, Yale University School of Medicine, New Haven, CT 06520–8034, USA. H. Zhang is in the Department of Epidemiology and Public Health, Yale University School of Medicine, New Haven, CT 06520–8034, USA.

*To whom correspondence should be addressed at Department of Genetics, M322, Stanford University School of Medicine, Stanford, CA 94305–5120, USA.